Original Research Article

Distribution, population structure, and fishery potential of the golden deep-sea crab, *Chaceon somaliensis* in the Kenyan Coast in East Africa

.

ABSTRACT

Aim: This study focused on *Chaceon somaliensis*, a species in the Geryonid family, which is commonly found in the Horn of Africa. The species has global commercial value, yet little is known about it. The study adds to our understanding of the species by identifying its distribution, population structure, and fisheries potential in the Kenyan Coast.

Methodology: Maxent modeling assessed the appropriate environmental variables and predicted potential species distribution and hotspot locations. Regression was used to explain *C. somaliensis* distribution and some aspects of the population structure.

Study design: Analytical

Results: Stratification by depth was observed with large male crabs (CW>150 mm, weight=1100 g) found in shallower depths (depth<501 m), while females, smaller in size (CW=92 mm, weight=316 g), seemed to prefer higher depths of >500 m. The Males were dominant (0.94), and females and juveniles comprised only 0.06 of the population. The population was found to be skewed towards males of large size (CW> 140 mm, weight 1100 g). Bathymetry and environmental variables associated with feeding and nutrients, such as phytoplankton, iron, and silicate, were the best predictors of species presence. Potential sites occurred on a ridge at gentle slopes (0.98°– 4.31), with the hotspot areas being spatially about 3,230 km^2 of 61,694 km^2.

Conclusion: The fishery was considered productive and suitable for maintaining marine biodiversity (catch> 94% adults). The male population should be monitored as it is the key indicator of the status of the fishery.

Keywords: Geryonid, Chaceon somaliensis, species distribution, Maxent, habitat modelling, Kenya

1. INTRODUCTION

The brachyuran family Geryonidae, characterized by its five anterolateral carapace teeth (1,2), is globally distributed in the continental slopes of the world's oceans (3,4) at depths 200–1500 m. Geryonidae are a source of food and supports numerous world commercial fisheries (3,5–7). The family comprises of four genera and twenty-four species (7) Those which have attracted scientific research include *Chaceon fenneri, Chaceon affinis, Chaceon macphersoni, Chaceon maritae, Chaceon quinquedens, Chaceon chilensis, Chaceon gordonae, Chaceon albus* and *Chaceon notialis* of the South West Atlantic Ocean (2,5,8–15). The *Chaceon* genus attains medium to large size, from 118 mm to 170 mm carapace width, and is a source of food, livelihood, and revenue, supports industrial fisheries and has ecological value. The crabs form part of the benthic community (6,7,16) .

Chaceon somaliensis (17), a Geryonid crab found and exploited in the Coast of Kenya is the interest of this research. The name *C. somaliensis* was derived from the locality as it was originally discovered, off-Somalia Coast, in the Horn of Africa (18). The crabs are large in size, with males generally being larger than the females (2,12). *C. somaliensis* crabs in Kenya are commercially harvested yet, little is known about it. This lack of information hinders conservation efforts (19). For instance, in Kenya, the reported export revenue of *C. somaliensis* was (USD $4,840, 26,400 and 37,100) for the years 2018, 2019 and 2020, whereas the exported quantities were (1,210, 6,600, and 6,100 kg) respectively. The reported live sea crabs' total catches were 55,065 and 109,746 kg for 2019 and 2020 (GoK, unpublished statistical reports), yet little was known about the fishery.

Previous studies of Geryonid crabs point to different factors that influences the crab's distribution and population structure. These include; ocean depth (5,7,13,20–22), indicators of food, such as chlorophyll-a (20,23,24), temperature, infaunal biomass (20), dissolved oxygen (25) mud content, and estuary bed height (23)), ontogenetic shift, and species interaction activities such as competition (24). Geryonid crabs also exhibited bathymetric migration of the females during the reproduction cycle (7). Stratification by depth was observed with depths of 400–500 m having higher biomass density, and abundance of the crabs and large-sized than in deeper regions of >600 m (5,21,26,27). Depth-sex stratification was also present, with males being larger and heavier than females and found in shallow places (optimum depth of 400–500 m). Females preferred deeper áreas >600 m (12,27). Geryonid crabs' weight also decreased with the increasing depth (5,7). This was attributed to large-scale ontogenetic migration, and that breeding population was restricted to the upper layers of the bathymetry range (5). This upscale migration of deep-sea crabs segregated by sex was observed for *Chaceon quinquedens, Geryon maritae,* and *Chionoecetes opilio* (20,28–30). Distribution and abundance were found to be highest in areas of canyons and slopes (5).

Geryonid crabs and other marine crab species studies have mostly focused on population data and ecological descriptions (5,16,21,31), (22). Surprisingly, as compared to terrestrial species distribution modelling (SDM) studies, there are still relatively few SDM studies in marine ecosystems (14,20,24,25,32–34). SDMs are models that characterize the relationship between species occurrence and environmental variables (35,36). Three main types of SDM exist, mechanistic, process-oriented and correlative models (15). Correlative SDM uses a self-learning algorithm without prior knowledge of the species to characterize its distribution (15,37,38). Correlative SDM is better suited to predicting species distribution in marine environments (24). The Maxent algorithm is an ideal correlative SDM algorithm (37,39). It produces areas with similar environmental conditions to the species prevalence areas, delineating potentially suitable sites (37,39–41). In earlier studies, Maxent outperformed other algorithms, such as the Genetic Algorithm for Rule Set Production (GARP) (42), and it worked well with only presence data. Maxent also produced easily interpretable outputs (34,43). Thus, species distribution models (SDM) were vital in informing ecosystems (19).

To the best of our knowledge, this is the first comprehensive study of *C. somaliensis* in the Kenyan Coast, and it provides new insights into population structure and species spatial distribution, environmental correlates, and fishery. This study takes a holistic approach employing regression analysis for population structure and SDMs to characterize the spatial distribution and environmental correlates of *C. somaliensis* in the marine environment. The research findings can help policymakers and fishery authorities implement efficient benthic species management methods, hence enhancing conservation efforts for the *Chaceon somaliensis* species. The analysis methods presented here could be used to investigate and provide information to improve management and control distribution, population structure, and fishery potential of other deep-sea crab species in other parts of the world.

2. MATERIAL AND METHODS

2.1. Site description

The Kenyan Coast study area elongates from the South Coast in Kwale County to the North Coast in Lamu County (Fig. 1). It extends from (-1.68°E, 41.97°S and -4.82°E and 39.36°), and it approximates 63,094 km^2. The Area experiences two primary seasons in a year caused by the monsoon wind: The North East Monsoon (NEM) winds from November to March and the South East Monsoon (SEM) winds starting from April to October (14,44). The region encompasses the North Kenya Banks, a region with rich fishery potential (45,46). Fig. 1 presents the Kenyan Coastal area and the occurrence areas of *Chaceon somaliensis* for 2019, 2020, and 2021. Fishing activities were mainly concentrated off-Kilifi, with less fishing off-Lamu and Mombasa Coast. The depths extended from 250 m to 1250 m.

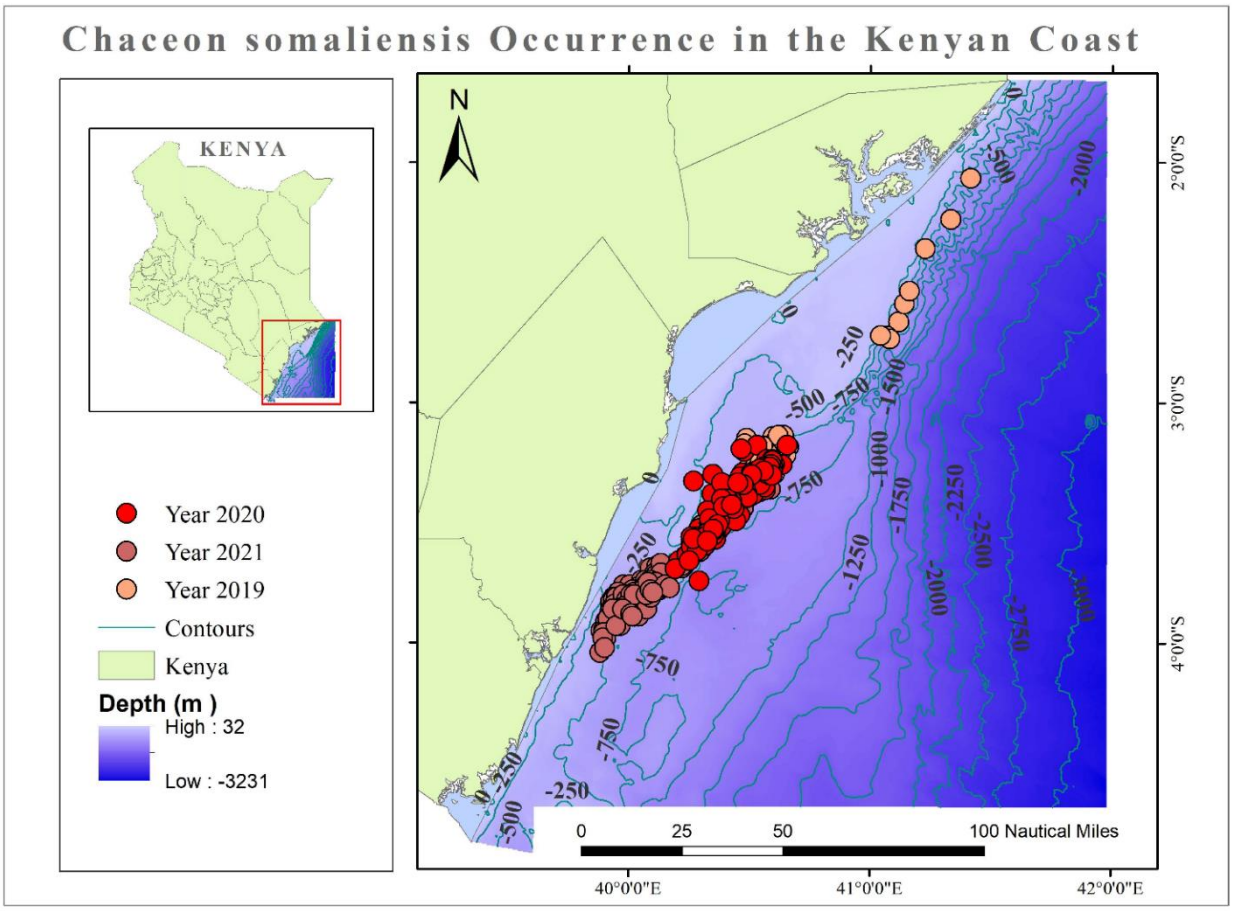

Fig. 1. Map of the Kenyan Coast with bathymetric contours and occurrence data of *Chaceon somaliensis* for 2019, 2020 and 2021.

2.2. Species sampling and analysis

The 2021/2022 occurrence data on *Chaceon somaliensis* was collected onboard a longline trap fishing vessel of over 25.56 m and a gross tonnage of 79 tons. The fishing equipment consisted of cylindrical pots/traps that had a diameter of 90 cm and a height of 40 cm and

were particularly effective for catching benthic crabs (47). The trap frames were metallic and were covered with a fishing net of 6 cm mesh size and had three openings made by use of mesh having different colors from the rest of the trap and were located at the mid-height of the trap. The trap-longlines', referred to as sets had an average length of 8,300 m and an average number of traps (337 traps), with each trap being placed at 20 m equidistance from the other. The longline-trap vessel fished for live crabs. The live captured crabs were stored in oxygenated water chambers with a temperature range of between 8.4°C to 12°C. Active data collection for morphometrical details took place onboard the fishing vessel from August 31, 2021, to January 16, 2022. A total of 44 out of 161 sets were sampled, with 1363 individuals of the deep-sea crab measured, one specimen in each pot translating to 1363 pots sampled for the deep-sea crab out of a total of 15,751 pots. The live crabs were first identified visually using crustacea standard indicators (14) to be *Chaceon somaliensis* and checked if all appendages were intact (3,27); the crabs were then placed on a flat measurement table ready for measurements. Immediately after being measured, the crabs were released into the oxygenated chambers. Random sampling method was used as it best captured the spatial and population variability of the fishery. The sets, traps and the crab in each trap were selected randomly. The place or fishing grounds to be sampled were limited to where the vessel fished. However, this did not affect the accuracy of the results when tested for sampling biases**.**
Measurements sizes of carapace width (CW) and carapace length (CL) were taken to the nearest 0.1 mm (5,22) and weight to the nearest 1 g using a vernier calliper, 0.01 mm accuracy (27) and an electronic balance (1 g accuracy), respectively. Carapace width was measured between most exterior carapace spines; carapace length measurements were between the rostrum and the abdomen (48). Sex identification was made by mode of observation. The male sex was identified by its narrow, straight, and T-like and the female by its broad-roundish abdomens (22,49).
Chaceon somaliensis historical data for 2019 and 2020, was sourced from the Kenya Fisheries Service (KEFS) and Kenya Marine and Fisheries Research Institute (KMFRI). The data was mainly catch and was used to calculate catch trends, fishing effort, and seasonality with the 2021 presence record.

2.3. Data analysis and modelling

Regression and descriptive statistics were used to compute seasonal catches, vessel catch trends and catch per unit effort (CPUE) to describe the species population. The catch rate (CPUE) was calculated as total catch (kg)/the number of traps (7,26) for the three years (2019, 2020, and 2021). Average catch details for 2019, 2020, and 2021 were calculated per set (total catch in kilograms/total number of sets). This was because using a total number of sets standardized the effects of hauling disruptions, vessel breakdowns, and lost traps compared to the use of time. Catch for the respective months during active data collection in 2021 was also analyzed. It should be noted that the fishing effort, weighted catch per unit effort (WCPUE), was introduced for the year 2021 (only when analyzing the 2021 catch in isolation) and was computed as:

$$WCPUE = \frac{t}{T} * CPUE \quad \text{.....(i)}$$

$$CPUE = \frac{rc}{ast} \quad \text{.....(ii)}$$

Where *t* represents the number of traps (in this case, *t*= 300), *T* represents the total number of traps, *rc* represents retained catch (kg), and *ast* represents averaged soak time (hrs.)

WCPUE was important to reduce the effect of the number of pots/traps on the total catch and CPUE in general. The WCPUE formula formulated by this research assumed 300 traps as the standard number of traps in a set. The 300 number of pots/traps was informed by the average number of pots being 334, the minimum number of pots being 186, and the maximum of 480 pots. CPUE was calculated using processed catch (7). WCPUE was able to be calculated for

the year 2021 because three parameters: catch weight, number of traps, and soak time were collected. WCPUE was a standardized fishing effort taking into account both the number of traps and soak time, hence a best-suited measure of fishing effort. WCPUE and CPUE were positively correlated.
Depth analysis was computed using a depth stratum of 100 m (5,21,22,47). The relationship between depth and catch, fishing effort, distance to the shore, sex, size, and seasonality was computed using Excel 2016 (50) and Statistica 12 (51) see (Fig. 2).

2.4. Environmental variables selection

Benthic environmental variables of averaged depth for the present period (2000–2014) were obtained from the Bio-ORACLE data portal https://bio-oracle.org/faq.php (52,53). As climate is a long-term measure of daily climatic conditions, it was less likely that the predictors had since changed to significantly affect this research. The variables were the monthly averaged conditions. The bathymetric data layer was acquired from the GEBCO's gridded bathymetric data set https://www.gebco.net (54). Altogether, sixty-nine raster layers were obtained for this study.

Twelve environmental variables were used, each with six distinct categories (maximum, mean, minimum, LT. maximum, Lt. Minimum, and range). *Lt.max and Lt.min were the averages of the maximum or minimum records per year* (see Table 1, (52,53). The bathymetric grid layer of 2022 (54), with a resolution of 15 arcseconds, formed the second data set.
Table 1 Benthic environmental variables adapted from the Bio-ORACLE data (https://www.bio-oracle.org/).

Layer	Unit	Max	Mean	Min	Lt. Max	Lt. Min	Range
Temperature	ÂºC	Yes	Yes	Yes	Yes	Yes	Yes
Salinity	PSS	Yes	Yes	Yes	Yes	Yes	Yes
Currents velocity	m-1	Yes	Yes	Yes	No	Yes	Yes
Nitrate	mol.m-3	Yes	Yes	Yes	Yes	Yes	Yes
Phosphate	mol.m-3	Yes	Yes	Yes	Yes	Yes	Yes
Silicate	mol.m-3	Yes	Yes	Yes	Yes	Yes	Yes
Dissolved molecular oxygen	mol.m-3	Yes	Yes	Yes	Yes	Yes	Yes
Iron	umol.m-3	Yes	Yes	Yes	Yes	Yes	Yes
Chlorophyll	mg.m-3	No	Yes	Yes	Yes	Yes	Yes
Phytoplankton	umol.m-3	Yes	Yes	No	Yes	Yes	Yes
Primary productivity	g.m-3.day-1	Yes	Yes	Yes	No	Yes	Yes
Light at bottom	-	Yes	Yes	Yes	Yes	Yes	Yes

*Yes - the predictor was available and downloaded. No - the predictors were not available

2.5. Preprocessing

Spatial data (bathymetry, environmental variables) was processed using ArcGIS 10.7 (55), with Excel spreadsheet software and Statistica 12 used for statistical work. The raster dataset's pixel size, spatial resolution, and projection were set to 0.833, 9.2 km, the same as the environmental variable from Bio-Oracle (52,53), and UTM projection zone 37S to match and for further processing in Maxent. The layers were then converted to the necessary ASCII format and used as the predictor environmental variable. At the same time, occurrence data from the statistical analysis (Fig. 2) was used as input occurrence points. Species distribution modeling was conducted using Maxent (42,43). Variable percentage contribution was used to

select high-weight environmental variables in influencing the *Chaceon somaliensis* species distribution. Once the environmental variables were established, they were further modeled to visualize the species' ecological hotspots.

2.6. Model Calibration

Maxent version 3.44 was used to compute species distribution models, also known as ecological niche modeling (39,56–58). Maxent was set to random sampling and used 70% of the data for training and 30% for the test. The output was set to logistic output, the threshold rule was set to minimum training presence, and other settings were left at default. Iterative modeling was done to identify suitable environmental predictors, with percentage contribution (%C) used to eliminate variables with 0% contribution. Six rigorous runs were done. When all variables had percentage contributions greater than 0 (%C >0), the process ended. The resulting predictors were picked as the most suitable for *Chaceon somaliensis* distribution. The first run involved all 69 predictors. Potentially suitable sites were then modeled using the established environmental variables and the occurrence points with the Maxent setting set to 10 replicates and replicate types to cross-validate. This was to produce an average model out of the ten replicas, increasing model predicting accuracy.

2.7. Model evaluation

The accuracy of the model was assessed using the receiver operating characteristics curve (ROC) and the Area Under the Curve (AUC) (25,39,57). AUC> 0.9 signify excellent accuracy, AUC 0.7–0.9 signifies moderate accuracy, and AUC < 0.7 signify poor accuracy (38). The maximum AUC achievable is 1, and an AUC above 0.5 in a model was considered to have performed better than in a random model (37). In evaluating the most important predictors influencing *Chaceon somaliensis* occurrence, the percentage contribution column was used to select the most important predictors (Fig. 2, %C>0).

2.8. Model outputs

Maxent outputs included weighted environmental predictors ranked, showing each predictor's percentage contribution to the model's overall performance (59). With the jackknife setting activated, Maxent weighed each variable contribution to the model's gain. The other outputs included response plots which were used to describe the tolerance limits of *C. somaliensis* to each variable. The plots showed each variable effect on the species being plotted and a final potential distribution model (60).

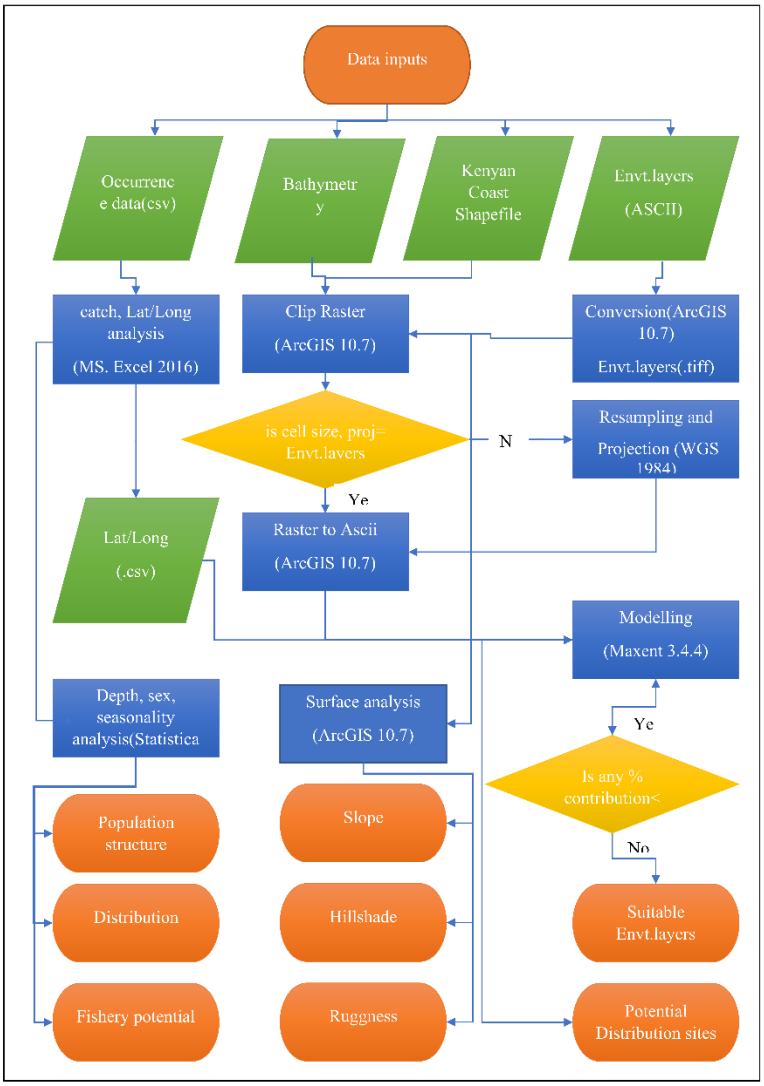

Fig. 2. The methodology of determining the population structure and species distribution modelling.

3. RESULTS AND DISCUSSION

3.1. Population structure and size distribution

Generally, *Chaceon somaliensis* catch decreased for the period of data collection, September to January 2022 (Fig. 3A); the decline and slight increase were attributed to the change in WCPUE during that period. Fishing effort (WCPUE) was positively correlated with the catch (R^2 = 0.94, P=0.02) for 2021 and R^2 =0.83, P=1.96^{-98} (CPUE) for the three years, 2019, 2020 and 2021. Fishing effort WCPUE calculated for 2021 was correlated with CPUE (R^2 =0.92). The population was skewed towards the males (0.94:0.05:0.01) for male, female, and immature crabs, respectively. The males were large and heavier compared to the females (Fig. 3B, mean CW = 143.94 ± 18.30 mm SD, mean CW = 92.1 ± 19.02 mm SD and 1077.05 ± 316.59 g SD) and (258.73 ± 323.18 g SD for M and F respectively) and with a mean (mean CW = 143.94 ± 18.30 mm SD) for the whole population depicting that only large crabs were

caught by the traps. The relationship between CW and weight was significant ($R^2 = 0.9$, P = 0.00). An exponential relationship curve was observed (Fig. 3C), and a normal weight distribution curve with two peaks (1000 and 1200 g) was observed (Fig. 3D). The mean soak time was 78 hours.

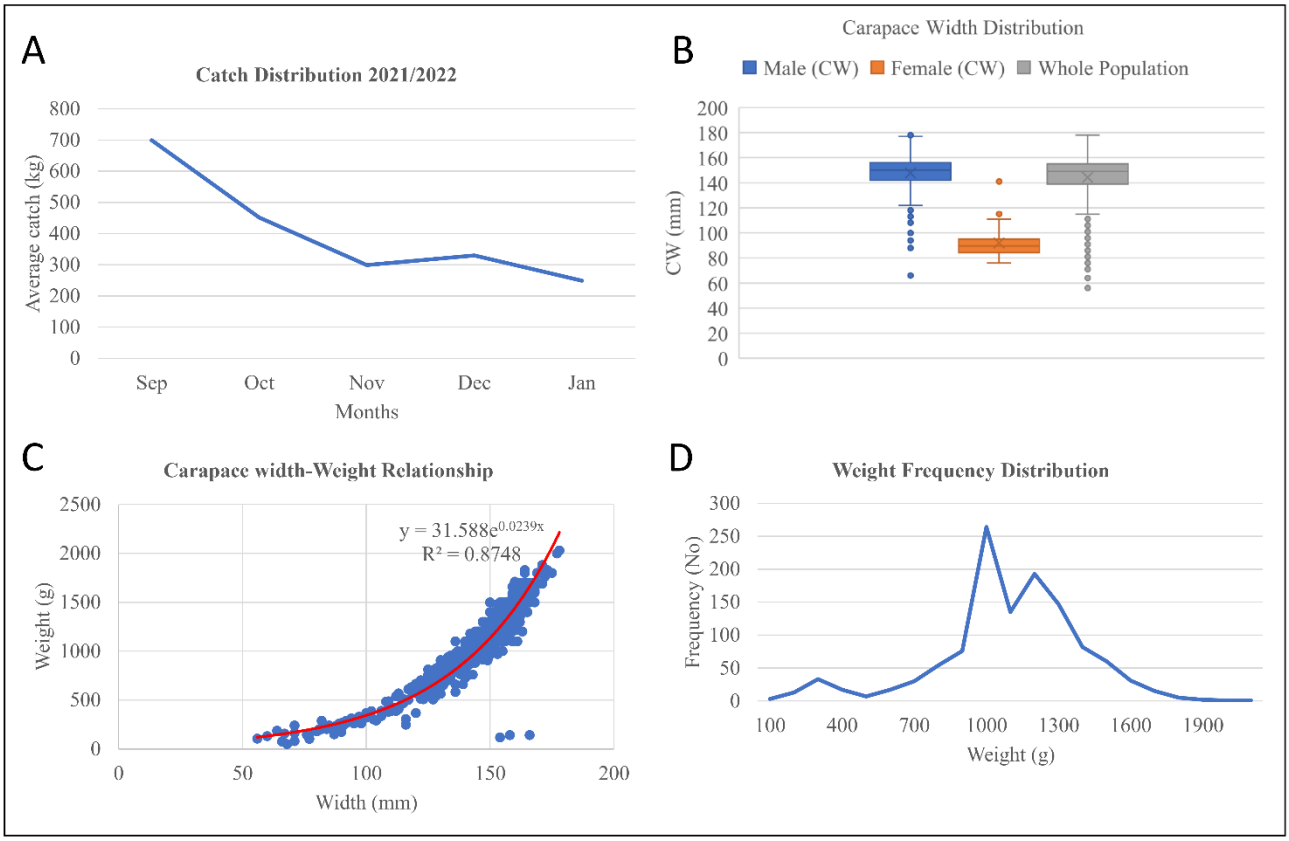

Fig. 3. Catch distribution 2021/2022 (A), carapace width distribution (B), carapace width-weight relationship (C), and weight frequency distribution (D).

3.2. Depth-Distribution, and Population Structure

Generally, *Chaceon somaliensis* catch and fishing effort decreased with an increasing depth in all the plotted 100 m depth horizons except for the depth 701–800, where the catch and fishing effort was higher than the depth range of 601–700 m (Fig. 4A). The depth was subdivided into 100 m (Attrill et al.,1990), and the catch was analyzed using those depth horizons (fishing depth range was from 395–759 m). Fishing distance from the shore increased with the increasing depth except for the same depth strata 701–800 m (Fig. 4B). For depth size (Fig. 4C and D), size generally decreased across the increasing depth profile except for the depth range 401–500 m, where the largest crab size of approximately 1.1 kg and carapace width of 151 mm were caught, polynomial relationship curve was observed. For the sex-depth distribution, the male and female abundance in relationship to depth was extremely opposite of each other ((Fig. 4E AND F)). The male sex crab followed the depth size distribution described above, with the depth (401–500) m having the highest abundance (see Fig. 4E). The females' abundances increased with the increasing depth, except for depth (401–500) m, where there was a zero abundance (see Fig.4F).

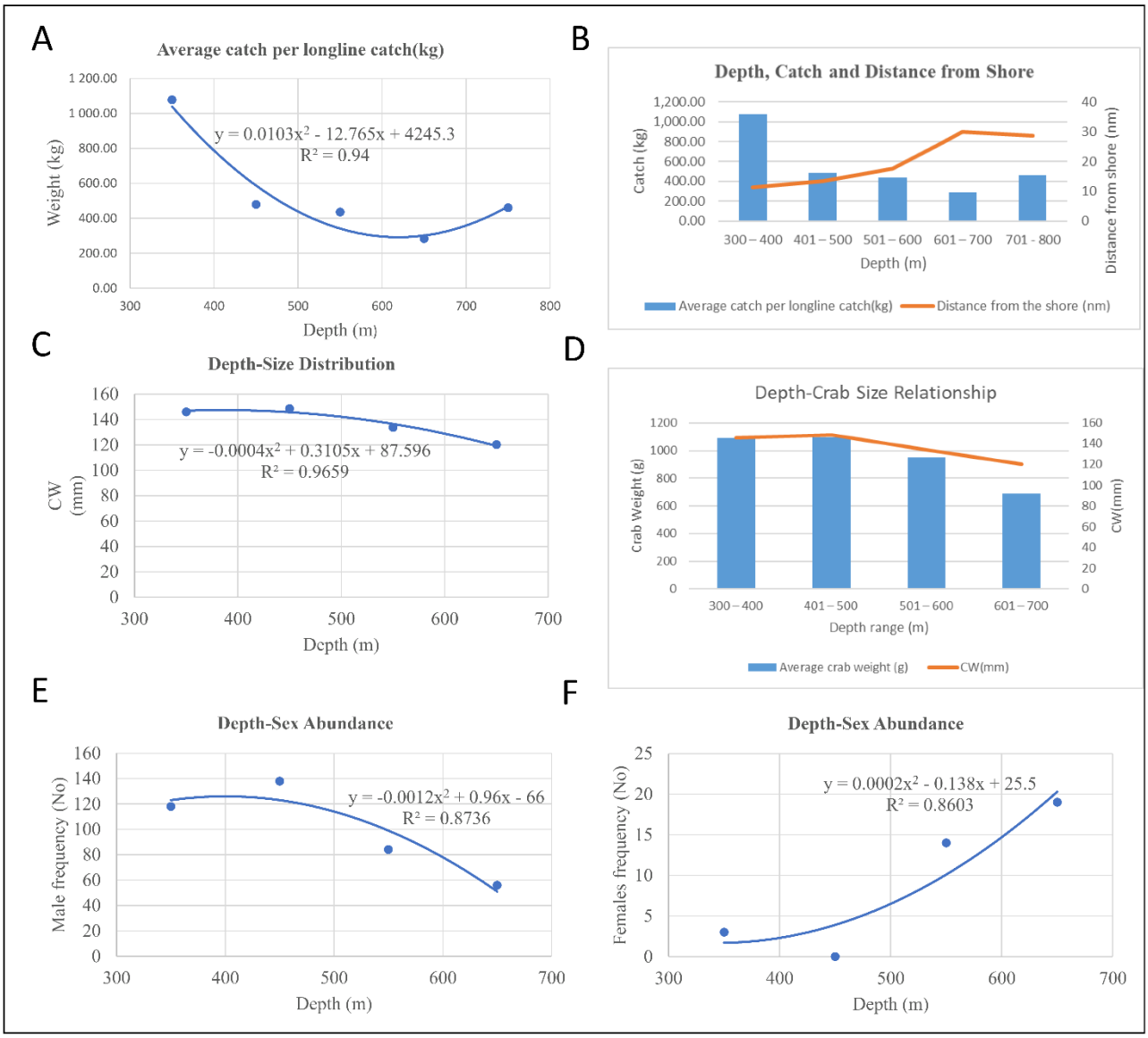

Fig. 4. *Average catch per longline (A), relationship between depth, catch and distance from shore (Fig. B), depth size distribution (Fig. C and D) Depth -sex relationship (Fig. 4E and F).*

3.3. Distribution and Seasonality

The fishing effort and the catch were high in NEM compared to SEM, with only an exception in 2021 (Figs. 5A and 5B). There was a decline in the fishing effort and catch and an increase in the fishing depth in the NEM season across the years (Figs. 5B, 5A, and 5C). Higher catches in the SEM season in 2021 can be attributed to the increased fishing effort, shallower fishing depth, and fishing closer to the shore (Figs. 5A, 5B, 5C, and 5D). CPUE, in this case, was calculated as catch (kg) / No of traps for comparison across the three years.

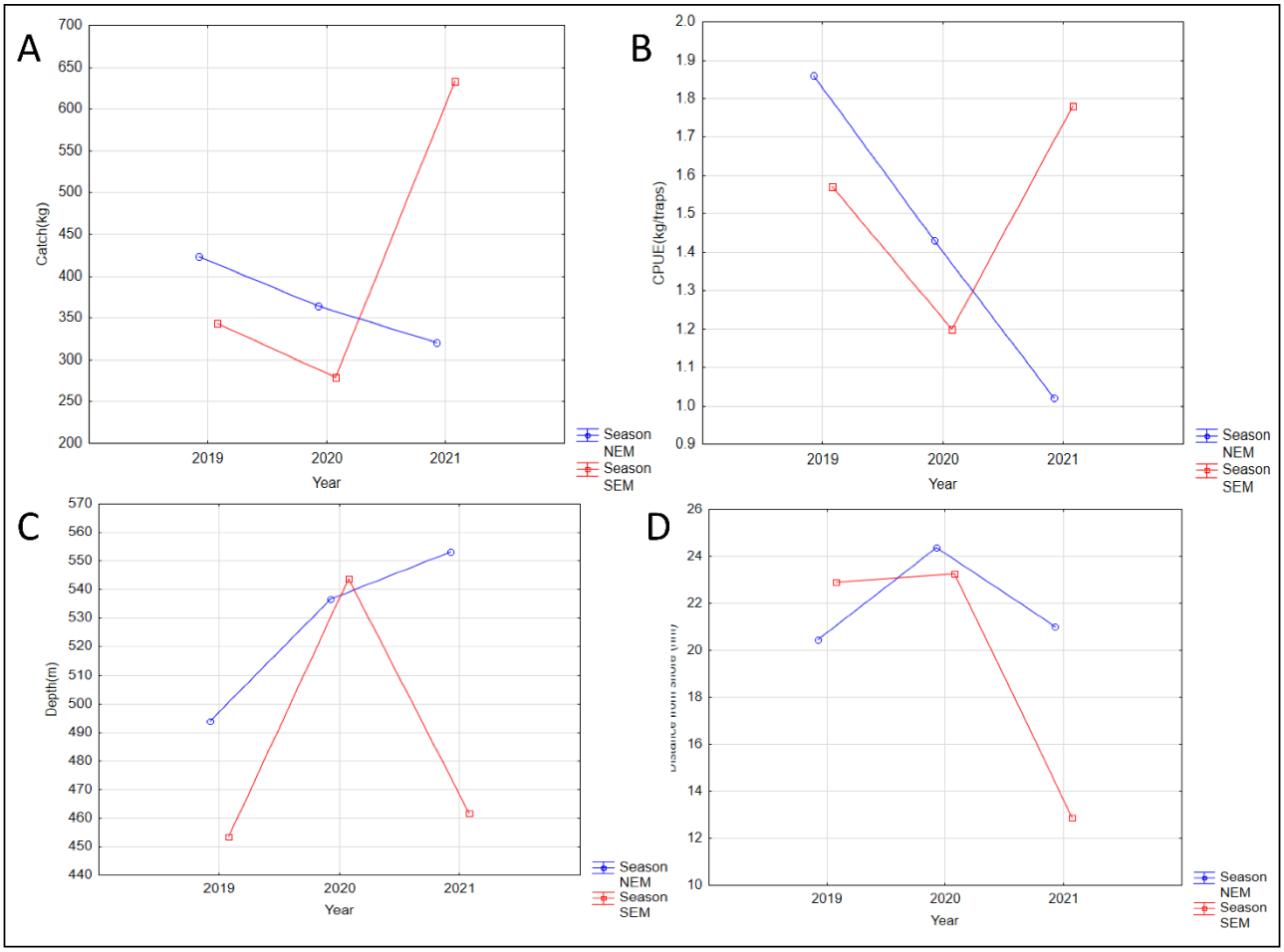

Fig. 5. Seasonality and catch per line (kg) (Fig. 5A), seasonality and CPUE (Fig. 5B), seasonality and fishing depth (Fig. 5C), seasonality and fishing distance (Fig. 5D).

3.4. SDM in the environmental variable evaluation

The predictors were rigorously modelled in Maxent to evaluate environmental variables influencing *Chaceon somaliensis* distribution on the Kenyan Coast. A set of 6 runs were done, with the first run having all the predictors (69). The selection of the most suitable variable was based on percentage contribution. Any variable whose percentage contribution was zero was eliminated, and the modeling process was redone till all variable contributions were more significant than 0%. In the fifth run (Table 2), all the remaining environmental variables had a percentage contribution of greater than 0%.

Table 2 Results of the *Chaceon somaliensis* species' fifth run of Maxent modeling.

Variable (Fifth run results)	Percentage contribution	Permutation importance
Mean phytoplankton	46.3	0.1
Silicate range	26.2	1
Mean primary productivity	5.6	0.1
Range of dissloved oxygen	5.3	4.1
Minimum LT currents speed	4.5	5.3

Variable (Fifth run results)	Percentage contribution	Permutation importance
Maximum LT chlorophyl	4.4	2.4
Iron range	4	11.5
Bathmetry	1.6	61.6
Mean silicate	1	11.7
Minimum iron	0.8	1.8
Maximum silicate	0.3	0
Minimum currents speed	0.2	0.3

All variables had a percentage contribution greater than zero in the fifth run. All variables measuring the same elements were eliminated to avoid overfitting, except the variable with the highest % contribution. Thus, silicate mean, iron minimum, currents velocity minimum, and silicate maximum were eliminated. The remaining seven variables were then rerun in the Maxent model. The model's outcome produced the environmental variables approximating the necessary conditions for *Chaceon somaliensis* occurrence, distribution, and population (Table 3).

Table 3 Environmental variables affecting the species distribution on the Kenyan Coast.

Variable	Percentage contribution	Permutation importance
Mean phytoplankton	47.5	0.8
Silicate range	25.7	2
Range of dissolved oxygen	5.6	4.7
Mean primary productivity	5.4	0.2
Maximum LT chlorophyl	5.1	3
Minimum LT currents speed	4.5	6.3
Iron range	4.1	6.3
Bathymetry	2	76.6

The seven environmental variables and the 1-bathymetry layer were the most suitable.

Fig. 6 shows the jackknife measure of variable importance when a variable is run in isolation and other variables omitted. Iron range had the highest gain showing that it had the most useful information. The variable that decreased the gain most when omitted was currents LT minimum, meaning it had very important information that the other variables did not.

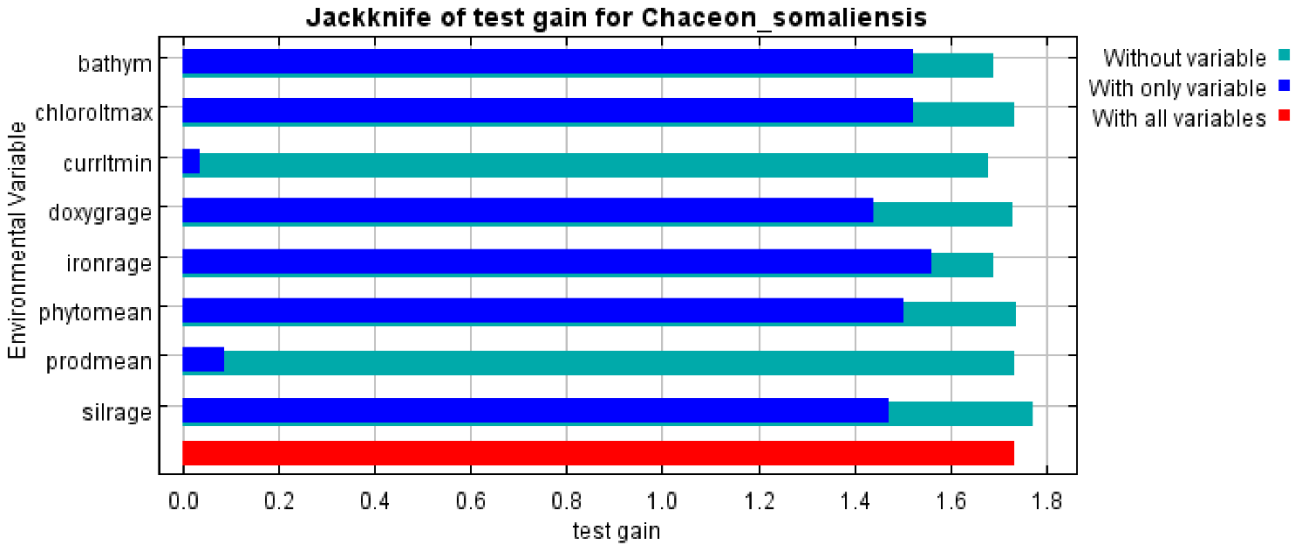

Fig. 6. *Jackknife measure of variable importance*

3.5. Variable optimum and tolerance limits

Suitable bathymetric depth ranged from approximately 100–500 m, with the peak of suitability to *C. somaliensis* occurrence being at 400 m depth (Fig. 7A). Chlorophyll exhibited a drastic rise and a narrow optimum peak at 0.01 mg/m^3 (Fig. 7B). The suitability range of minimum currents LT velocity to *Chaceon somaliensis* was between 0.002–0.08 m/s (Fig. 7C). Dissolved molecular oxygen suitability ranged from 20 mol/m^3 to 57 mol/m3 (Fig. 7D), iron range to *Chaceon somaliensis* was from 0.4 umol/m^3 to 0.7 umol/m^3(Fig. 7E), mean phytoplankton suitability range was narrow, 0.02 umol/m^3 (Fig. 7F), suitability range of silicate range was between 8 mol/m^3 to 18.2 (Fig. 7H), mol/m^3 with 18 mol/m^3 representing the optimum conditions.

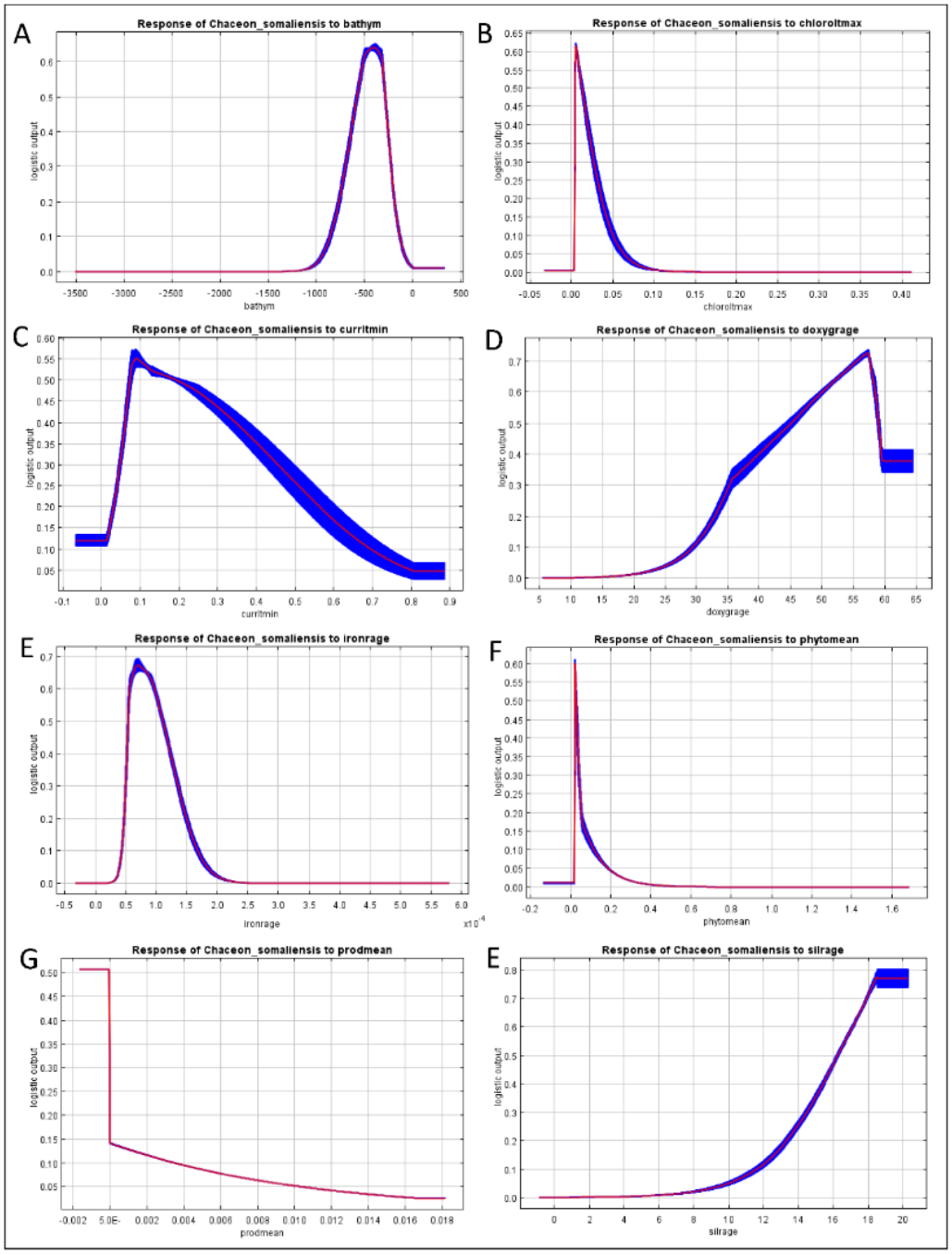

Fig. 7. The *Chaceon somaliensis* response curves for the environmental predictors.

The eight variables selected (Table 3) were modeled in Maxent to produce the potential distribution areas. Maxent setting for this exercise was set to 10 iterations. The random test percentage was set to 0 to allow random partitioning between train and test data in each replica.

3.6. Potential sites and hotspot areas

Potential sites for *Chaceon somaliensis* showed a latitudinal distribution from the Southwest Coast of Kenya to the Northeast direction. The distribution followed the North Kenya Banks ridge from the South Coast of Kenya towards the Northeast, with the depth of the ridge extending from 250 m to 1250 m (Figs. 8A and 8B). Hotspot areas of great abundance of the species coincided with the ridge (Fig. 9B). The hotspot zone was approximately 3,230 km^2 of 61,694 km^2 of the study area (Fig. 8B).

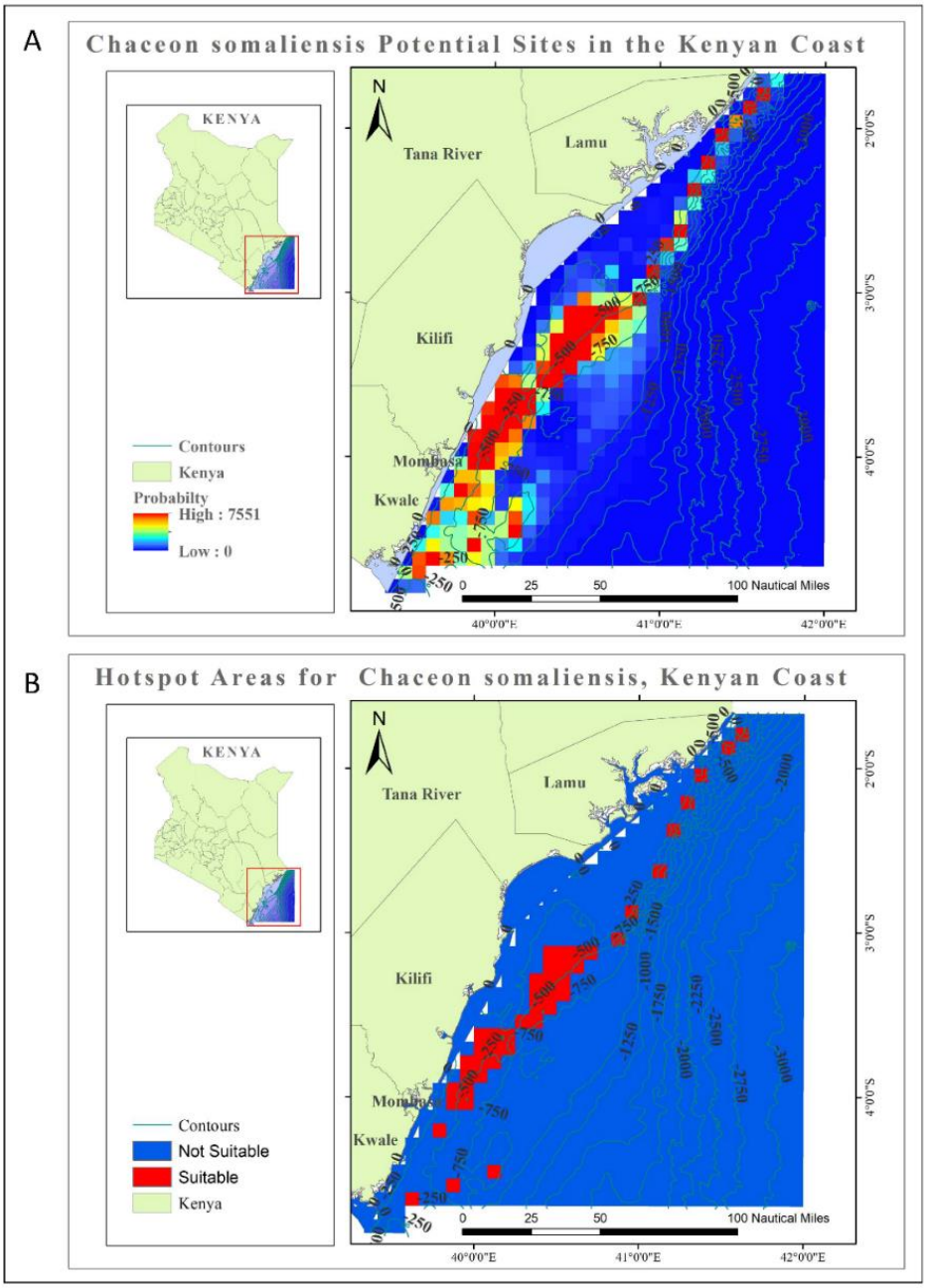

Fig. 8. (A) Potential sites, (B) hotspot areas, red colour show potentially suitable sites for *Chaceon somaliensis* occurrence, blue colour colors represent areas of low suitability.

Overlaying the raster image of the potential sites with raster images of the slope, hill shade, and ruggedness showed that the hotspot areas occur at slopes (5,20) with an angle between 0.98° and 4.31° within a low hill shade and a low rugged terrain (Fig. 9AD)

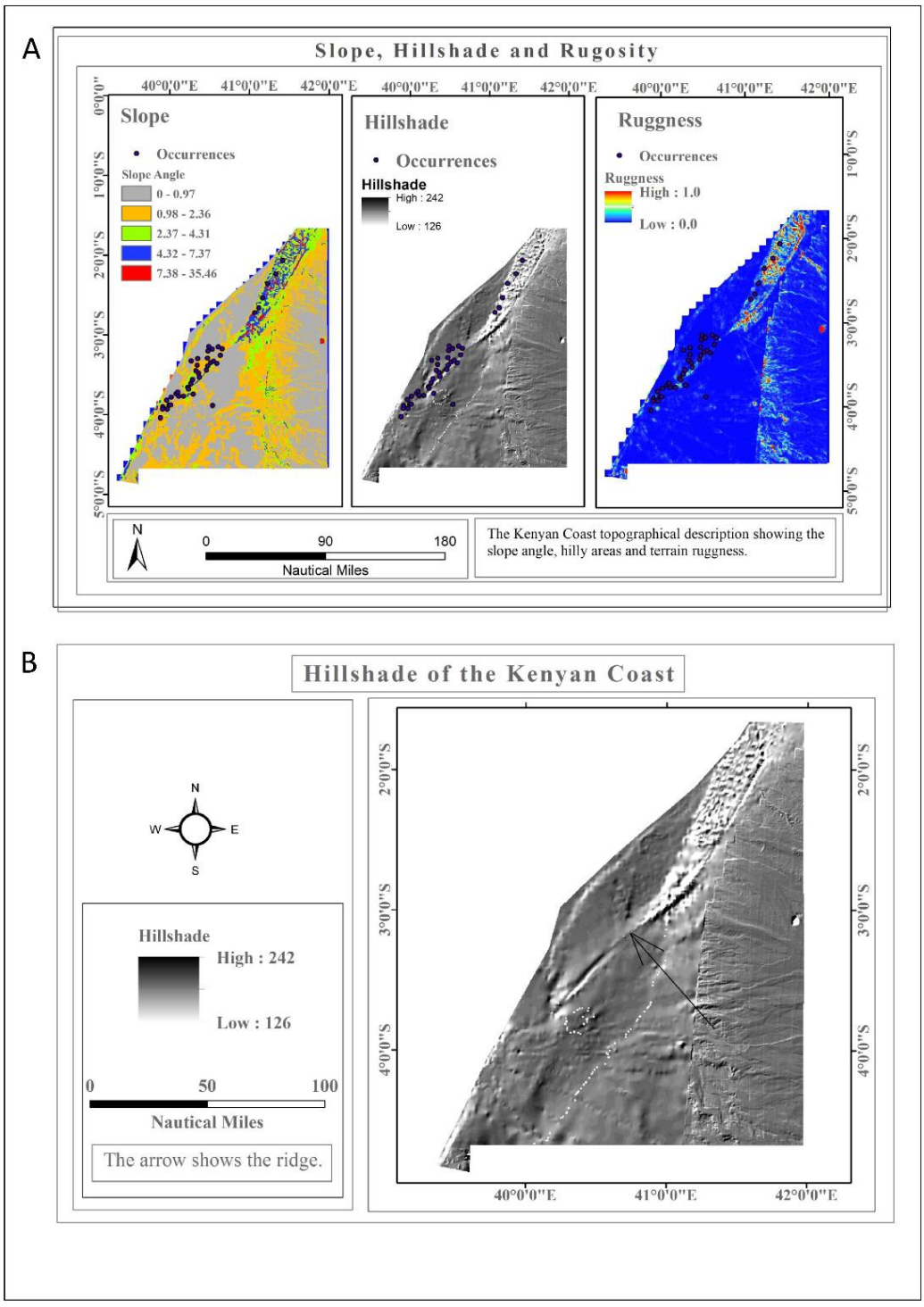

Fig. 9. (A) Hillshade and rugosity of *Chaceon somaliensis* potential distribution sites. (B) ridge-like depression running along the Kenyan Coast, Slope.

3.7. Accuracy of the model

For the above model, the average AUC for the ten replicates was 0.938 ± 0.022 SD (Fig. 10A). Models for the respective three years using each year's occurrence data were developed to compare the effect of sampling on the model output over the overall potential site model above (Fig. 10B).

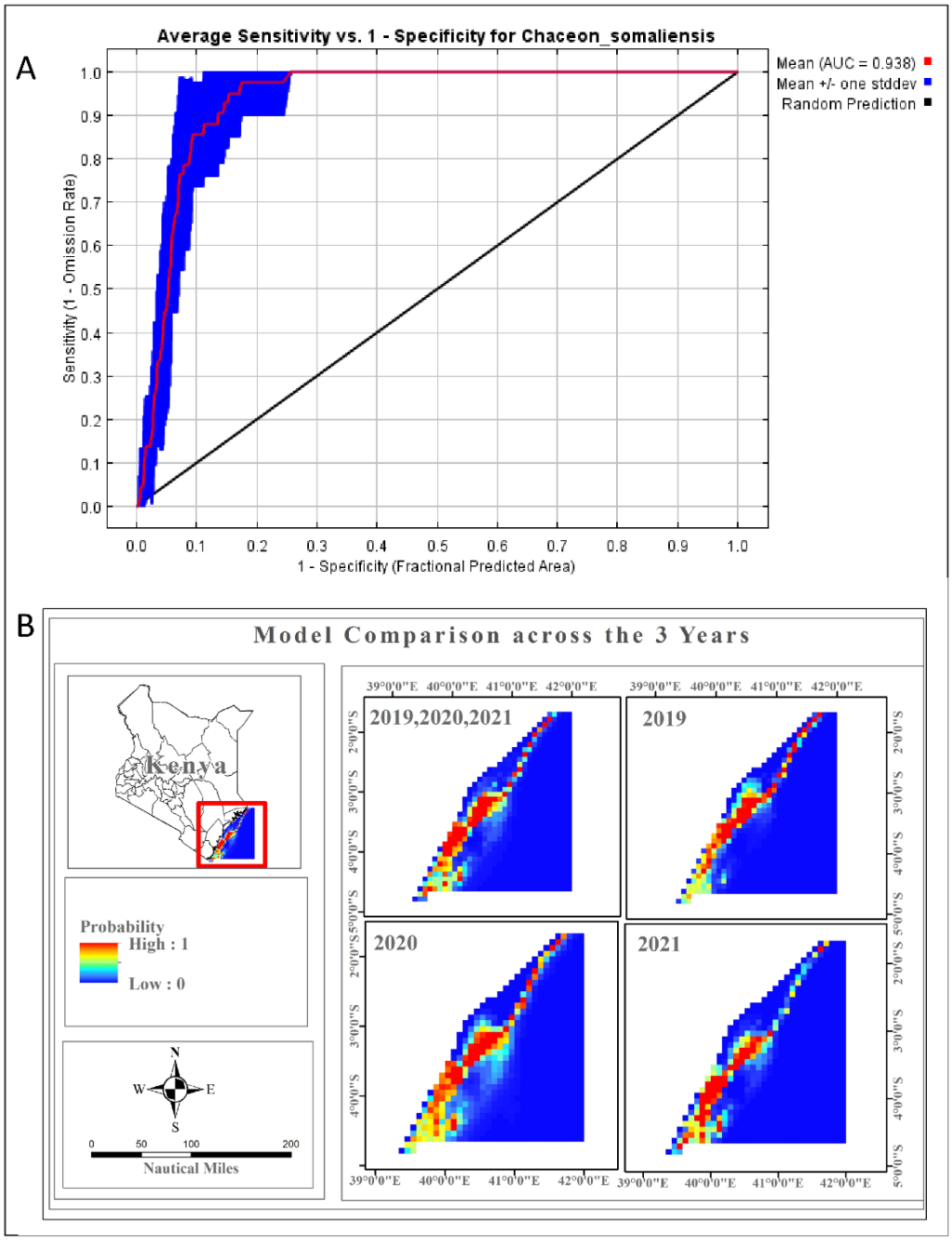

Fig. 10. AUC curve of *Chaceon somaliensis* (Fig. 10A) and comparison maps among models with the first model (2019, 2020, 2021) being the overall model, the same as (Fig. 10B).

The output (Fig. 10B) shows there was a negligible effect of sampling on the overall performance of our model. The 3-year model, 2019, 2020, and 2021, can also be used to calibrate environmental variables to specific grounds of the Kenyan Coast as they showed that the percentage contribution and permuted importance of primary production was 0% for both in all the years showing that primary production was not an important predictor and could be left out when running future models. Maxent train AUC and test AUC for the years 2019, 2020, and 2021 were 0.9, 0.964 and 0.975, 0.964 and 0.905, and 0.979 and 0.943, respectively, exhibiting high accuracy (38).

4. DISCUSSION

Chaceon somaliensis population abundance was found to be skewed towards large-sized male crabs. The population abundance was typical of Geryonid crabs (12). This was also evidenced by the Geryonid *Chaceon chilensis* making up 97.9 of the sampled population in Robinson Island, Chile (12), *Chaceon gordonae* (1:0.82) for M: F in Brazil (27). In contrast, female *Chaceon macphersoni* were dominant (1:0.29) in the KwaZulu–Natal Coast of South Africa (6). Possible reasons for male dominancy include the low mobility in the females, thus making it difficult to enter the traps, and soaking time-which would allow the small female crabs to escape (61). Fishing method and sampling bias might also be the reasons for males' dominance (62). This was because, in the use of traps as fishing gear, ovigerous females tended to avoid traps when brooding and sampling bias in that smaller crabs avoided entering the traps when larger crabs were present (62).

Chaceon somaliensis males were larger and heavier than the females (mean CW = 143.94 ± 18.30 mm SD), (mean CW = 92.1 ± 19.02 mm SD) and (1077.05 ± 316.59 g SD), (258.73 ± 323.18 g SD) for males and females respectively. This was common for Geryonid crabs (12), *Chaceon gordonae* males were larger (mean CL = 110.81 ± 14.52 mm SD) and heavier (650.39 ± 236.26 g SD) than females mean CL and weight, respectively= 102.00 ± 16.55 mm SD and 387.42 ± 151.89 g SD (27), *Chaceon fenneri* (3,21), *Chaceon affinis* (4) and *C. macphersoni* CW. 121.3 mm v 101.0 mm (6). (63) in the study of *C. maritae* attributed this characteristic of the males being larger than the females to the difference in molting patterns between the sexes, with the females having a shorter molting period in the immature stage and longer after maturity. Another deep-sea crab, not of Geryonid family, such as *Chionoecetes opilio* (in the Gulf of St. Lawrence), had similar characteristics, with males being abundant and larger than the females CW=154 ± 12.5 mm and 118.6 ± 12.1 mm for M and F respectively (26). Notably, *C. Somaliensis* in this study were comparatively larger than the other Geryonid, with the abundance of the species occurring above a carapace width of 140 mm and a bi-modal weight distribution curve (at 1000 and 1200 g, see Fig 3D) observed. Thus, based on size, the traps mainly caught adult crabs. This and the positive correlation between CPUE and catch (r2 =0.83, p=1.96E-98), made an 'ideal distribution' (26), showing the fishery's healthy status.

Segregation by depth was observed for *C. somaliensis*, both depth-abundance and depth-sex stratification. The bathymetric layer from Maxent modelling (Fig. 7A and 4D) showed the depth stratification with an optimum depth range of 401–500 m. Depths <500 m had large-sized male crabs and numerical abundance. Females' abundance increased with depth, with the highest abundance at depths 601–700 m. This sex stratification was also observed for other Geryonid crabs; in the Atlantic, *Chaceon fenneri* males occurred in depths 274–549 m and females 733–823 m (64), *Chaceon affinis* in the Azores also exhibited similar patterns (65). In other studies, the sex-stratification differed, and males predominated over deeper zones and females' shallower ones, *C. notialis* with the females being abundant in shallower regions 300–400 m (47), and *C. fenneri* in Brazil had females found in deeper zones compared to the males (7). Segregation by sex was also observed for *C. gordonae* in Brazil (27). The possible explanation

for the depth-sex stratification was the difference in the reproduction cycle between males and females (7) or because of environmental and biological conditions (27). Depth-abundance stratification was also evident for *C. gordonae* at depths 400–500 m (27), *C. macphersoni* abundance increased with increasing depths 200–499 m and declined thereafter (6), *Chaceon notialis* depths 400–700 m (47), *Geryon trispinosus*, occurred at depths 506 and 510 m (5). Depth stratification was also observed for the snow crab, *Chionoecetes opilio* where males were dominant in all the depth strata (100–700 m) but abundance increased at depth>400 m (26) In contrast, (4) and (12) provided deeper depth strata as the regions of abundance, *C. affinis* abundance occurred at strata (600–799 m) and (800–899 m) and mean sizes decreased with depth for both sexes and for *Chaceon chilensis* depth at 750 m and the species was larger at deeper strata's compared to the shallow ones.

Distribution of *C. somaliensis* decreased with increasing distance from the shore. This was because as the distance to the shore increased, depth also increased, and as depth and *C. somaliensis* were inversely related, so was the distance to the shore. For seasonality during NEM (November to March), the distribution of fishing effort and the catch was higher than in SEM (April to October) seasons for the two years (2019 and 2020). This compares with (6) observed seasonality in the distribution of *Chaceon macphersoni,* with the highest catch in November and December and lowest in June and July for trawl catch, probably of the catch was higher in spring and lowest in winter. (47) also observed seasonality for *C. notialis* where abundance occurred in summer (December–February, in Argentinian-Uruguayan area) possibly too because of the higher fishing effort during that time (CPUE of approximately 25kg per trap). The possible reason for the change in seasonal catch (higher catch during SEM than in NEM) in the year 2021 for this research was due to the increased fishing effort (Fig. 5B), the vessel fished in shallower regions (Fig. 5C) and closer to the shore (Fig. 5D). Though, 3-year data might not have been adequate to conclude on seasonality.

In the evaluation of environmental predictors suitable for *Chaceon somaliensis* distribution, it was found that factors related to food (20,24) and nutrient minerals were the top predictors (Table 3). These include mean phytoplankton, range of silicate, maximum Lt chlorophyll, and mean primary productivity. Depth was observed to be an important variable in influencing the distribution of the species, with a permutation importance of 76.6 % (Table 3), meaning that depth by itself had useful information for the distribution of the *Chaceon somaliensis*, which other predictors did not have (42,43). The tolerance limit of *Chaceon somaliensis* to each environmental variable differed, with the species having a wide niche breadth for bathymetry, dissolved molecular oxygen, and silicate. Other variables suitable for *Chaceon somaliensis* distribution included minimum LT current velocity, dissolved molecular oxygen, and iron range (Table 3). Though temperature and salinity were considered very important in the distribution of deep-sea crabs, this study found the most important input factors related to feeding, nutrients and bathymetry (5).

Hotspot areas and potential zones occurred in the North Kenya Bank ridge with a slope angle of between 0.98° and 4.31° and a low rugged terrain. This compares with other Geryonid crabs, *Chaceon gordonae* found on the ridge of Sierra Leone, off Western Africa and the Mid-Atlantic ridge in the Brazilian Archipelagos of Saint Paul and Peter (27,66). (21) explained the habitats of Geryonid crabs as varied, ranging from sloppy areas, valleys at depths of 200–900 m having and or soft sandy bottoms, rocky escarpments, sinkholes, boulder and slab areas, vertical escarpments and dense coral thickets. The need for species to migrate easily or the effect of sediment type on the habitat of the species (67) and the crab's ability to detect steep slopes and migrate to low slopes a behavior termed as negative geotaxis (5) were cited as the reasons for the Geryonid crabs' habitat choice.

The Maxent SDM confirmed most of the statistical results; the optimum depth for the species distribution (400–500 m) aligned with the statistical results. The model also tried to explain the observed distribution with food, nutrients and depth (topography) variables influencing the species population structure and its geographical distribution. The SDM also pointed out the optimum conditions under which the species thrived. Potential hotspot areas that only covered a small fraction of the study are (0.05), emphasizing the need for sustainable exploitation and conservation of the resources. The SDM potential sites model should guide conservation and potential efforts towards Kenya's emerging *Chaceon somaliensis* fishery.

4. CONCLUSION

The study could not emphasize enough the importance of integrating statical analysis and SDM in evaluation species population structure and its distribution properties. It showed the complementary nature of the two methods, with both SDM and statistics used to achieve the main objective. Regression analysis and SDM established that the *Chaceon Somaliensis* population followed a depth stratification, with shallow areas having both large and heavier crabs. Both the Maxent model and statistical analysis suggested that the optimal depth for the species was found at depths 400–500 m. The Maxent SDM further evaluated potential environmental variables found in the study and their influence on the species distribution, migration and population. Eight environmental variables were suggested as of importance in influencing the distribution of the species in the study area. The model also produced the potential suitable areas and their topographic characteristics. The study agreed with (5) that the species was prone to gentle slopes and ridges (along the slopes of the North Kenya Banks). It also brought into focus the small size of the hot spot areas (3,230 km^2) a very important information in the conservation practices of the species. Annual limits catch for the species can be introduced as a conservation measure. For instance, in the sea off Eastern Florida, the annual catch limit for *C. fenneri* was set at 909,090 kg whole weight. The limit could be modified for the fishery after conducting a stock survey to help in the conservation of the deep-sea crab fishery in Kenya. Effective monitoring practices that use population structure, depth, and predictive models as key system elements should be implemented (38,40). This study agrees with previous studies (12,27) that the male population sustains the Geryonid fishery and should be factored in the management and conservation of the fishery.

Among other contributions of this study was in profiling the new *Chaceon somaliensis* fishery, providing its population structure and distribution and using SDM to evaluate environmental variables and model the potential suitable sites. This information can be used to conserve and manage the new fishery. The study also helped correctly identify and name the deep-sea crab as *Chaceon somaliensis*; previous unpublished data referred to the species as *Chaceon fenneri.* The newly introduced fishing effort (WCPUE) should be tested for its rigidity in future research of a similar nature. Though the study is essential, it did not cover the role of sediment size in influencing the distribution of the species*, Chaceon somaliensis* molting patterns, maturity, reproduction, life cycle, and biology and habitat types (6,21,27).

REFERENCES

1. Manning and Holthuis - TWO NEW GENERA AND NINE NEW SPECIES OF GERYONID CR.pdf.

2. Ferreira et al. - 2016 - First record and preliminary information on the bi.pdf.

3. Trigg C, Perry H. Size and Weight Relationships for the Golden Crab, Chaceon fenneri, and the Red Crab, Chaceon quinquedens, from the Eastern Gulf of Mexico. Gulf Res

Rep [Internet]. 1997 Jan 1 [cited 2023 Jul 11];9. Available from: http://aquila.usm.edu/gcr/vol9/iss4/11

4. Biscoito M, Freitas M, Pajuelo JG, Triay-Portella R, Santana JI, Costa AL, et al. Sex-structure, depth distribution, intermoult period and reproductive pattern of the deep-sea red crab Chaceon affinis (Brachyura, Geryonidae) in two populations in the north-eastern Atlantic. Deep Sea Res Part Oceanogr Res Pap. 2015 Jan;95:99–114.

5. Attrill MJ, Hartnoll RG, Rice AL, Thurston MH. A depth-related distribution of the red crab, Geryon trispinosus (Herbst) [= G. tridens Krøyer]: indications of vertical migration. Prog Oceanogr. 1990;24(1–4).

6. Groeneveld JC, Everett BI, Fennessy ST, Kirkman SP, Santos J, Robertson WD. Spatial distribution patterns, abundance and population structure of deep-sea crab Chaceon macphersoni, based on complementary analyses of trap and trawl data. Mar Freshw Res. 2013;64(6):507–17.

7. Barros Carvalho T, De Oliveira Filho RR, Da Cruz Lotufo TM. Note on the fisheries and biology of the golden crab (Chaceon fenneri) off the northern coast of Brazil. Lat Am J Aquat Res. 2009 Nov 10;37(3):571–6.

8. Manning RB, Holthuis LB. Geryon fenneri, a new deep-water crab from Florida (Crustacea: Decapoda: Geryonidae). Proc Biol Soc Wash [Internet]. 1984 [cited 2024 Jun 7]; Available from: https://repository.si.edu/bitstream/handle/10088/8760/SMS-Manning-1984.pdf

9. ROBERT B, ERDMAN NJB, JosEPH JT. CH4CEON FENNERI AND C. QUINQUEDENS (BRACHYURA: GERYONIDAE). Comp Biochem Physiol. 1991;99(3):383–5.

10. Erdman et al. - 1991 - Oxygen consumption of the deep-sea crabs Chaceon f.pdf.

11. Davie et al. - 2007 - A new species of deep-sea crab of the genus Chaceo.pdf.

12. Guerrero A, Arana P. Size structure and sexual maturity of the golden crab (Chaceon chilensis) exploited off Robinson Crusoe Island, Chile. Lat Am J Aquat Res. 2009;37(3):347–60.

13. Gutiérrez NL, Masello A, Uscudun G, Defeo O. Spatial distribution patterns in biomass and population structure of the deep sea red crab Chaceon notialis in the Southwestern Atlantic Ocean. Fish Res. 2011 Jun;110(1):59–66.

14. Everett BI, Groeneveld JC, Fennessy ST, Dias N, Filipe O, Zacarias L, et al. Composition and abundance of deep-water crustaceans in the Southwest Indian Ocean: Enough to support trawl fisheries? Ocean Coast Manag. 2015 Jul 1;111:50–61.

15. Melo-Merino SM, Reyes-Bonilla H, Lira-Noriega A. Ecological niche models and species distribution models in marine environments: A literature review and spatial analysis of evidence. Ecol Model. 2020 Jan 1;415.

16. Da Silva Cortinhas MC, Ortega I, De Souza Alves Teodoro S, Proietti M, Masello A, Kersanach R, et al. Defining deep-sea fishery stocks through multiple methods: The case of the red crab Chaceon notialis Manning & Holthuis, 1989 (Crustacea, Decapoda,

Geryonidae) in the Southwestern Atlantic. Deep Sea Res Part Oceanogr Res Pap. 2022 Jan;179:103659.

17. Manning - A NEW DEEP-SEA CRAB, GENUS CHACEON, FROM THE ARABI.pdf.

18. Manning B. A NEW DEEP-SEA CRAB, GENUS CHACEON, FROM THE ARABIAN SEA (CRUSTACEA, DECAPODA, GERYONIDAE).

19. Grüss A, Drexler MD, Chancellor E, Ainsworth CH, Gleason JS, Tirpak JM, et al. Representing species distributions in spatially-explicit ecosystem models from presence-only data. Fish Res. 2019 Feb;210:89–105.

20. Hardy SM, Lindgren M, Konakanchi H, Huettmann F. Predicting the distribution and ecological niche of unexploited snow crab (Chionoecetes opilio) Populations in alaskan waters: A first open-access ensemble model. In: Integrative and Comparative Biology. 2011. p. 608–22.

21. Reed JK, Farrington S, Messing C, David A. Distribution and Habitat Use of the Golden Crab Chaceon fenneri off Eastern Florida Based on in situ Submersible and ROV Observations and Potential for Impacts to Deep Water Coral/Sponge Habitat. Gulf Caribb Res. 2017;28:1–14.

22. Capezzuto F, D'Onghia G, Carluccio A, Maiorano P. Distribution and life strategy of the deep-sea crab Paromola cuvieri (Risso, 1816) (Brachyura, Homolidae) in the central Mediterranean Sea over twenty-five years. Deep Sea Res Part Oceanogr Res Pap. 2023 Jun;196:104002.

23. Ysebaert T, Herman PM. Spatial and temporal variation in benthic macrofauna and relationships with environmental variables in an estuarine, intertidal soft-sediment environment. Mar Ecol Prog Ser. 2002;244:105–24.

24. Robinson LM, Elith J, Hobday AJ, Pearson RG, Kendall BE, Possingham HP, et al. Pushing the limits in marine species distribution modelling: Lessons from the land present challenges and opportunities. Glob Ecol Biogeogr. 2011 Nov;20(6):789–802.

25. Georgian SE, Anderson OF, Rowden AA. Ensemble habitat suitability modeling of vulnerable marine ecosystem indicator taxa to inform deep-sea fisheries management in the South Pacific Ocean. Fish Res. 2019 Mar;211:256–74.

26. Swain DP, Wade EJ. Spatial distribution of catch and effort in a fishery for snow crab (Chionoecetes opilio): Tests of predictions of the ideal free distribution. Can J Fish Aquat Sci. 2003 Aug;60(8):897–909.

27. Ferreira RCP, Nunes DM, Shinozaki Mendes RA, Pires AMA, Hazin FHV. First record and preliminary information on the biology of the deep sea African crab, Chaceon gordonae (Ingle, 1985) (Brachyura: Geryonidae) in Saint Peter and Saint Paul Archipelago, Brazil. Lat Am J Aquat Res. 2016 May 10;44(2):392–400.

28. Melville-Smith R. Density distribution by depth of *Geryon maritae* on the northern crab grounds of South West Africa/Namibia determined by photography in 1983, with notes on the portunid crab *Bathynectes piperitus*. South Afr J Mar Sci. 1985 Jun;3(1):55–62.

29. Beyers C de B, Wilke CG. Quantitative stock survey and some biological and morphometric characteristics of the deep-sea red crab Geryon quinquedens off South West Africa. Fish Bull-Contrib Oceanogr Fish Biol-South Afr Dept Ind Sea Fish Branch. 1980;

30. Haefner Jr PA. Seasonal aspects of the biology, distribution and relative abundance of the deep-sea red crab Geryon quinquedens Smith, in the vicinity of the Norfolk Canyon, western North Atlantic [Internet]. Available from: https://scholarworks.wm.edu/vimsarticles/1263

31. Davie PJF, Ng PKL, Dawson EW. A new species of deep-sea crab of the genus Chaceon Manning & Holthuis, 1989 (Crustacea: Decapoda: Brachyura: Geryonidae) from Western Australia. Zootaxa. 2007 Jun 14;1505(1):51–62.

32. Serrano A, González-Irusta JM, Punzón A, García-Alegre A, Lourido A, Ríos P, et al. Deep-sea benthic habitats modeling and mapping in a NE Atlantic seamount (Galicia Bank). Deep-Sea Res Part Oceanogr Res Pap. 2017 Aug 1;126:115–27.

33. Ben Rais Lasram F, Hattab T, Nogues Q, Beaugrand G, Dauvin JC, Halouani G, et al. An open-source framework to model present and future marine species distributions at local scale. Ecol Inform. 2020 Sep 1;59.

34. Holmes M, Kotta J, Persson A, Sahlin U. Marine protected areas modulate habitat suitability of the invasive round goby (Neogobius melanostomus) in the Baltic Sea. Estuar Coast Shelf Sci. 2019 Nov;229:106380.

35. Guisan A, Zimmermann NE. Predictive habitat distribution models in ecology [Internet]. Vol. 135, Ecological Modelling. 2000 p. 147–86. Available from: www.elsevier.com/locate/ecolmodel

36. Gábor L, Jetz W, Zarzo-Arias A, Winner K, Yanco S, Pinkert S, et al. Species distribution models affected by positional uncertainty in species occurrences can still be ecologically interpretable. Ecography. 2023 Jun;2023(6):e06358.

37. Pearson RG. Species' Distribution Modeling for Conservation Educators and Practitioners.

38. França S, Cabral HN. Predicting fish species distribution in estuaries: Influence of species' ecology in model accuracy. Estuar Coast Shelf Sci. 2016 Oct;180:11–20.

39. Hallstan S. Species distribution models. Ecol Appl Manag Biodivers Fac Nat Resour Agric Sci Dep Aquat Sci Assess Upps Swed [Internet]. 2011 [cited 2024 Jun 6]; Available from: http://pub.epsilon.slu.se/8131/1/hallstan_s_110519.pdf

40. Li M, Zhang C, Xu B, Xue Y, Ren Y. Evaluating the approaches of habitat suitability modelling for whitespotted conger (Conger myriaster). Fish Res. 2017 Nov;195:230–7.

41. Bittner RE, Roesler EL, Barnes MA. Using species distribution models to guide seagrass management. Estuar Coast Shelf Sci. 2020 Aug;240:106790.

42. Phillips SJ, Dudík M, Phillips SJ. Modeling of species distributions with Maxent: new extensions and a comprehensive evaluation.

43. Phillips SJ, Anderson RP, Schapire RE. Maximum entropy modeling of species geographic distributions. Ecol Model. 2006;190(3–4):231–59.

44. Jebri F, Jacobs ZL, Raitsos DE, Srokosz M, Painter SC, Kelly S, et al. Interannual monsoon wind variability as a key driver of East African small pelagic fisheries. Sci Rep. 2020 Aug 6;10(1):13247.

45. Jacobs ZL, Jebri F, Raitsos DE, Popova E, Srokosz M, Painter SC, et al. Shelf-Break Upwelling and Productivity Over the North Kenya Banks: The Importance of Large-Scale Ocean Dynamics. J Geophys Res Oceans. 2020 Jan 1;125(1).

46. Morgans JFC. The north Kenya banks. Nature. 1959;184(4682):259–60.

47. Defeo O, Little V, Barea L. Stock assessment of the deep-sea red crab Chaceon notialis in the Argentinian-Uruguayan Common Fishing Zone. Vol. 11, Fisheries Research. 1991 p. 25–39.

48. Anam R, Mostarda E. FIELD IDENTIFICATION GUIDE TO THE LIVING MARINE RESOURCES OF KENYA.

49. Fernández-Vergaz V, Abellán LL, Balguerías E. Morphometric, functional and sexual maturity of the deep-sea red crab Chaceon affinis inhabiting Canary Island waters: chronology of maturation. Mar Ecol Prog Ser. 2000;204:169–78.

50. Microsoft Corporation. Microsoft Excel [Internet]. 2016. Available from: https://office.microsoft.com/excel

51. StatSoft Inc. STATISTICA (data analysis software system), version 12 [Internet]. 2014. Available from: http://www.statsoft.com

52. Tyberghein L, Verbruggen H, Pauly K, Troupin C, Mineur F, De Clerck O. Bio-ORACLE: a global environmental dataset for marine species distribution modelling: Bio-ORACLE marine environmental data rasters. Glob Ecol Biogeogr. 2012 Feb;21(2):272–81.

53. Assis J, Tyberghein L, Bosch S, Verbruggen H, Serrão EA, De Clerck O. Bio-ORACLE v2.0: Extending marine data layers for bioclimatic modelling. Glob Ecol Biogeogr. 2018;27(3).

54. GEBCO Compilation Group. GEBCO 2022 Grid. 2022.

55. ESRI. ArcGIS Desktop: Release 10.7. Redlands, CA: Environmental Systems Research Institute; 2011.

56. Aguirre-Gutiérrez J, Carvalheiro LG, Polce C, van Loon EE, Raes N, Reemer M, et al. Fit-for-Purpose: Species Distribution Model Performance Depends on Evaluation Criteria - Dutch Hoverflies as a Case Study. PLoS ONE. 2013 May 14;8(5).

57. SDMtoolbox JB. A python-based GIS toolkit for landscape genetic, biogeographic and species distribution model analyses., 2014, 5. DOI Httpsdoi Org1011112041-210X. 12200:694–700.

58. Guillera-Arroita G, Lahoz-Monfort JJ, Elith J, Gordon A, Kujala H, Lentini PE, et al. Is my species distribution model fit for purpose? Matching data and models to applications. Glob Ecol Biogeogr. 2015 Mar;24(3):276–92.

59. Nor W, Zainol Z, Abdullah @. HABITAT MAPPING AND SPECIES DISTRIBUTION MODELLING OF THE ENDANGERED BULLOAK JEWEL BUTTERFLY A thesis submitted by. 2016.

60. Obunga G, Siljander M, Maghenda M, Pellikka PKE. Habitat suitability modelling to improve conservation status of two critically endangered endemic Afromontane forest bird species in Taita Hills, Kenya. J Nat Conserv. 2022 Feb 1;65.

61. Barea L, Defeo O. Aspectos de la pesquería del cangrejo rojo (Geryon quinquedens) en la zona común de pesca argentino-uruguaya. Publ Com Téc Mix Fr Mar. 1986;1(1):38–46.

62. Taggart SJ, O'Clair CE, Shirley TC, Mondragon J. Estimating Dungeness crab (Cancer magister) abundance: crab pots and dive transects compared. 2004 [cited 2024 Jun 7]; Available from: https://aquadocs.org/handle/1834/30926

63. Melville-Smith R. A growth model for the deep-sea red crab (Geryon maritae) off South West Africa/Namibia (Decapoda, Brachyura). Crustaceana. 1989;279–92.

64. Lindberg WJ, Wenner EL. Geryonid crabs and associated continental slope fauna: a research workshop report. 1990 [cited 2024 Jun 7]; Available from: https://aquadocs.org/handle/1834/18134

65. Pinho MR, Gonçalves JM, Martins HR, Menezes GM. Some aspects of the biology of the deep-water crab, Chaceon affinis (Milne-Edwards and Bouvier, 1894) off the Azores. Fish Res. 2001;51(2–3):283–95.

66. Ingle RW. Geryon gordonae sp. nov.(Decapoda Brachyura, Geryonidae) from the northeastern Atlantic Ocean. Crustaceana. 1985;88–98.

67. Bluhm B, Iken K, Mincks Hardy S, Sirenko B, Holladay B. Community structure of epibenthic megafauna in the Chukchi Sea. Aquat Biol. 2009 Dec 8;7:269–93.